THE JOURNAL OF BIOLOGICAL CHEMISTRY
Vol. 279, No. 49, Issue of December 3, pp. 50764–50772, 2004
Printed in U.S.A.

Taz1 Binding to a Fission Yeast Model Telomere

FORMATION OF TELOMERIC LOOPS AND HIGHER ORDER STRUCTURES*

Received for publication, August 25, 2004
Published, JBC Papers in Press, September 21, 2004, DOI 10.1074/jbc.M409790200

Lubomir Tomaska‡, Smaranda Willcox§, Judita Slezakova‡, Jozef Nosek¶, and Jack D. Griffith§‖

From the Departments of ‡Genetics and ¶Biochemistry, Comenius University, Faculty of Natural Sciences, Mlynska dolina, 842 15 Bratislava, Slovakia and the §Lineberger Comprehensive Cancer Center and Department of Microbiology and Immunology, University of North Carolina, Chapel Hill, North Carolina 27599

Similar to its human homologues TRF1 and TRF2, fission yeast Taz1 protein is a component of telomeric chromatin regulating proper telomere maintenance. As mammalian TRF1 and TRF2 proteins have been shown to directly bind telomeric DNA to form protein arrays and looped structures, termed t-loops, the ability of Taz1p to act on fission yeast telomeric DNA in similar ways was examined using purified protein and model DNA templates. When incubated with Taz1p, model telomeres containing 3′ single-stranded telomeric overhangs formed t-loops at a frequency approaching 13%. Termini with blunt ends and non-telomeric overhangs were deficient in t-loop formation. In addition, we observed arrays of multiple Taz1p molecules bound to the telomeric regions, resembling the pattern of TRF1 binding. The presence of t-loops larger than the telomeric tract, a high frequency of end-bound DNAs and a donut shape of the Taz1p complex suggest that Taz1p binds the 3′ overhang then extrudes a loop that grows in size as the donut slides along the duplex DNA. Based on these *in vitro* results we discuss possible general implications for fission yeast telomere dynamics.

Telomeres, the DNA-protein complexes at the ends of linear chromosomes, stabilize the termini and protect them from end-to-end fusion. With a few exceptions, telomeres of most eukaryotic cells consist of an array of short repeats rich in guanines on the strand running 5′ to 3′ toward the chromosome end. Another general feature of nuclear telomeres is the presence of a 3′ overhang of the G-rich strand at the termini (reviewed in Ref. 1). It has been suggested that telomeres exist in at least two different states (2), they "open" to allow telomerase to access the end of the telomeric DNA and then "close" to protect chromosome ends from unwanted recombination and mask them from the double strand break repair systems. Changes from open to closed states would be mediated by specific protein components of the telomeric chromatin (3, 4).

Telomeric loops (t-loops)[1] formed by an invasion of the 3′ single-stranded (ss) overhang of mammalian telomeres into the duplex telomeric region (5) were suggested to hide the natural end of the chromosome and presumably reflect the closed state of the telomere. T-loops were subsequently found at the termini of micronuclear chromosomes of *Oxytricha nova* (6), at the telomeres of *Trypanosoma brucei* (7) and *Pisum sativum* (8), as well as at the ends of linear mitochondrial DNA of the yeast *Candida parapsilosis* (9), suggesting that they may represent an evolutionary ancient means of telomere maintenance (10). Recently Nikitina and Woodcock (11) demonstrated that mouse and chicken telomeres could be visualized in a t-loop structure following gentle isolation of the telomeres in a chromatinized state.

In the original study of mammalian t-loops it was found that the formation of loops is mediated by TRF2 protein (5). TRF2 and its homologue TRF1 were identified as proteins that bind double-stranded (ds) telomeric DNA as homodimers (12–14). Multiprotein complexes built around TRF1 and TRF2 have recently been identified with the TRF1 complex being implicated in telomere length regulation and the TRF2 complex in telomere protection (4, 15). The TRF-associated proteins include Tin2 (16), tankyrase (17), hRap1 (18), Werner and Bloom syndrome helicases (19), DNA polymerase β (20), and Pot1 and Pip1 (21).

Although TRF1 and TRF2 exhibit a high degree of homology, their role in telomere dynamics seems to be different, probably because of the differences at their N termini (22). In contrast to TRF2, TRF1 is unable to promote t-loop formation *in vitro*. Whereas TRF1 forms filamentous structures on telomeric repeat arrays and promotes parallel pairing of telomeric tracts *in vitro* (23), TRF2 induces t-loop formation and binds preferentially to the ss/ds junction at the 3′ telomeric overhang (24). A 5′-TTAGGG-3′ overhang of at least six nucleotides is required for loop formation. Termini with 5′ overhangs or blunt-ended ends are deficient in loop formation.

Saccharomyces cerevisiae with its powerful genetic and molecular biologic tools would seem to offer a valuable system for the detailed analysis of t-loop formation. Indirect genetic evidence suggests that telomeres in *S. cerevisiae* appear to form fold-back structures thus emphasizing telomere looping as a common theme in telomere architecture (25–28). However, it seems unlikely that the budding yeast telomeres form "true" t-loops. First, telomeric sequences in *S. cerevisiae* are very heterogeneous ($C_{2-3}ACA_{1-6}/T_{1-6}GTG_{2-3}$) (29, 30), which would decrease the probability that the 3′ telomeric overhang could invade into the double-stranded telomeric region based on base complementarity. In addition, the budding yeast genome does not contain a gene encoding a TRF-like telomeric protein. Rap1 protein contains its own Myb domain and seems to fulfill func-

* This work was supported in part by Fogarty International Research Collaboration Award TW05654-01, Howard Hughes Medical Institute Grant 55000327, Slovak agency VEGA Grants 1/9153/02 and 1/0006/03, and Comenius University Grant UK/131/2002. The costs of publication of this article were defrayed in part by the payment of page charges. This article must therefore be hereby marked "*advertisement*" in accordance with 18 U.S.C. Section 1734 solely to indicate this fact.

‖ Supported by an Ellison Senior Scholar Award and National Institutes of Health Grants GM31819 and CA19014. To whom correspondence should be addressed: Lineberger Comprehensive Cancer Center, University of North Carolina, Mason Farm Road CB7095, Chapel Hill NC 27599-7295. Tel.: 919-966-2151; Fax: 919-966-3015; E-mail: jdg@med.unc.edu.

[1] The abbreviations used are: t-loops, telomeric loops; ss, single-stranded; ds, double-stranded; Ni-NTA, nickel-nitrilotriacetic acid; nt, nucleotide(s).

tions divided between TRF proteins and hRap1p in mammalian cells (which lacks a Myb domain) (31, 32).

In contrast to *S. cerevisiae*, telomeric repeats of *Schizosaccharomyces pombe* are more regular with a consensus sequence 5′-GGTTACA-3′ (33). The length of the telomere, excluding the telomere associated sequences (TAS1, TAS2) is on average 300 bp. In addition, the fission yeast contains a TRF homologue (Taz1p) and similar to mammalian cells, spRap1 binds to the telomeres indirectly via Taz1p. In addition, the role of spRap1p seems to be restricted to telomeres and thus is distinct from that of scRap1p, which is involved in silencing at both the telomere and mating type locus (34). Therefore, fission yeast may provide a more relevant model for the study of TRF-mediated telomere transactions and the evolution of mammalian-like telosome.

Taz1p (telomere-associated in *Schizosaccharomyces pombe*) was originally found in a one-hybrid screen using telomeric DNA as a target (35). It shares homology to the Myb proto-oncogene DNA-binding domains present in both TRF1 and TRF2. In addition, similar to TRF1 and TRF2, it contains a centrally located sequence motif of about 200 amino acids, referred to as the TRF homology domain that is unique to this gene family and overlaps with a dimerization domain mediating strong homotypic interactions (14, 36). The possibility that Taz1p functions in fission yeast may encompass those of both hTRF1 and hTRF2 is consistent with the observation that the Myb domain and TRF homology domain of Taz1p are more homologous to hTRF1, whereas other regions of Taz1p show higher levels of homology with hTRF2 (37).

Disruption of the *taz1*$^+$ gene in *S. pombe* is not lethal and *taz1*$^-$ haploids grow vegetatively at the same rate as wild-type cells. Deletion of *taz1*$^+$ causes a roughly 10-fold increase in telomere length (35). However, despite the changes in telomere length, *taz1*$^-$ cells did not exhibit a decrease in viability after extensive subculturing (35). In contrast to vegetative growth, sexual reproduction of *taz1*$^-$ cells is aberrant because of defective meiosis (35). Detailed analysis of the role of Taz1p in meiotic division revealed that it is necessary for telomere aggregation adjacent to the spindle pole body during meiotic prophase. In the absence of Taz1p, telomere clustering at the spindle pole bodies is disrupted, meiotic recombination is reduced (3–10-fold), and both spore viability and the ability of zygotes to re-enter mitosis is impaired (38–40).

In addition to its role in meiosis, Taz1p is required for the repression of telomere-adjacent gene expression, most likely by establishing or maintaining a telosome structure (35). This hypothesis is supported by the observation that mating of *taz1*$^+$ and *taz1*$^-$ cells results in diploids, in which the telomeres remain longer than normal for many generations, although the telomere position effect is quickly restored. Importantly, Taz1p remains associated with subtelomeres even in the absence of telomeric repeats thus emphasizing its role in inheritance of telomeric chromatin (41).

Although the mitotic growth of *taz1*$^-$ cells is similar to wild-type under stress-free conditions, *taz1*$^-$ cells exhibit lethal telomere fusions when subjected to nitrogen starvation inducing an uncommitted G_1 state (42). The fusions are mediated by the Ku-dependent nonhomologous end joining pathway and are not dependent on homologous recombination (42). Taz1p is also essential for cell cycle progression at 20 °C, a temperature at which Δ*taz1* mutants exhibit a G_2/M checkpoint delay, chromosome missegregation, and double-strand DNA breaks (43). Thus, analogous to mammalian TRF2 protein, Taz1p helps provide a telomeric cap that prevents Ku from recognizing telomeres as double-strand breaks.

Similar to the *taz1*$^-$ mutant, the *rap1*$^-$ mutant of *S. pombe* is nonessential for mitotic growth, but leads to elongation of telomeres and defective meiosis. Cells disrupted for both *taz1*$^+$ and *rap1*$^+$ genes exhibit the same phenotype as single disruptants suggesting that they function in the same pathway(s) (44). Thus Rap1p of fission yeast binds to the telomere through interaction with Taz1p, paralleling that found in human cells (18).

Whereas the list of the fission yeast telomeric proteins has grown rapidly, their precise roles in establishing telomere architecture are still unknown. Using an *in vitro* reconstitution approach, we have begun to reconstitute the fission yeast telosome. We have generated a model telomere DNA containing a double-stranded array of consensus telomeric repeats (5′-GGTTACA-3′) and in which the ss overhang can be altered in sequence and length. Using this artificial telomere, we examined the ability of recombinant Taz1p to bind to this telomeric DNA *in vitro* and to organize the model telomeres into different structures. Both arrays of Taz1 bound along the telomere and t-loop forms were observed, pointing to the similarities between Taz1p and TRF1 and TRF2, and shedding more light on TRF-mediated telomere remodeling in all eukaryotic systems.

EXPERIMENTAL PROCEDURES

Enzymes and Oligonucleotides—Restriction enzymes, T4 polynucleotide kinase, T4 DNA ligase, calf intestinal phosphatase, and the Klenow fragment of *Escherichia coli* DNA polymerase I were from New England Biolabs (Beverly, MA) and were used according to the manufacturer's instructions. [γ-^{32}P]ATP (3000 Ci/mmol) was from ICN Biomedicals (Irvine, CA). Oligonucleotides were purchased from MWG Biotech Inc. (Greensboro, NC) or Invitrogen (Carlsbad, CA) and either contained a 5′ phosphate, or were phosphorylated by T4 polynucleotide kinase and unincorporated nucleotides were removed using a QIAquick nucleotide removal kit (Qiagen).

Construction of S. pombe Model Telomere DNA—A plasmid containing a block of fission yeast consensus telomere repeats 5′-GGTTACA-3′ flanked by asymmetric restriction sites for BbsI and BsmBI was constructed using the approach of Stansel *et al.* (24). Several cycles of telomeric track expansion resulted in a plasmid (pLT500) containing 74 telomeric repeats (518 bp). All plasmid constructs were propagated in *Escherichia coli* Sure2 cells (Stratagene, La Jolla, CA).

Ligation of Oligonucleotide Tails to pLT500—The plasmid pLT500 was digested with BsmBI and BamHI and dephosphorylated using calf intestinal phosphatase. Ligation reaction mixtures contained 3 μg of the linearized plasmid, a 5-fold molar excess of oligonucleotide, and 400 units of T4 DNA ligase in 50 mM Tris-HCl, pH 7.5, 10 mM $MgCl_2$, 10 mM dithiothreitol, 1 mM ATP, 25 μg/ml bovine serum albumin, and T4 DNA ligase (400 units). The free oligonucleotides were removed using a QIAquick PCR purification kit (Qiagen).

Purification of Recombinant Taz1p-His (Further Taz1p)—The bacterial strain overproducing Taz1 with an N-terminal His tag (pQE30 vector, Qiagen) and protocol for its purification on Ni-NTA Superflow agarose were provided by Dr. Julia P. Cooper (Cancer Research Institute, London, United Kingdom). For some preparations, Talon™ Metal affinity resin (Clontech, Palo Alto, CA) was employed instead of Ni-NTA. Typically, a protein extract from a 1-liter culture was loaded on 1 ml of the beads and the bound proteins were eluted stepwise with increasing concentrations (50–250 mM) of imidazole. The Taz1p containing fractions were dialyzed using a Slide-A-Lyzer cassette (Pierce) against 1 liter of 20 mM HEPES-NaOH, pH 7.5, 20% glycerol, 100 mM NaCl, 1 μg/ml leupeptin and stored at −20 °C. The fractions eluted from the nickel column contained two major bands migrating at apparent sizes of 90 and 70 kDa based on SDS-PAGE on a 10% gel (45). The two forms of Taz1p were separated by reloading the sample on the Ni-NTA column followed by elution with a gradient (50–250 mM) imidazole.

Mass Spectrometry—The precise molecular weights of Taz1p and a C-terminal truncated form were determined by Dr. Christoph Borcher in the University of North Carolina Michael Hooker Proteomics Core Facility using an Electrospray Ionization Quadrapole Time-of-flight Mass Spectrometer following in-gel tryptic digestion of the proteins (46).

Immunoblot Analysis—Proteins were separated by SDS-PAGE and electrotransferred to a nitrocellulose filter (BA85, Schleicher & Schuell) in a buffer containing 25 mM Tris, 192 mM glycine, pH 8.3, 20% meth-

anol for 60 min at 250 mA. Probing with the anti-penta(His) antibodies (Qiagen) and subsequent chemiluminescent assay using the BM Chemiluminescence Western blotting Kit (Roche Diagnostics) were performed according to the corresponding manufacturer's instructions.

Determination of Molecular Mass of Native Taz1p—The apparent molecular mass of native Taz1p was determined using gel filtration fast protein liquid chromatography on a Superose 6 column (Amersham Biosciences) equilibrated with 10 mM Tris-Cl, pH 7.4, 0.1 mM EDTA, 50 mM NaCl. The column was calibrated with apoferritin (440 kDa), catalase (240 kDa), aldolase (158 kDa), and bovine serum albumin (66 kDa).

Electrophoretic Mobility Shift Assay—To obtain a dsDNA probe the pLT126 plasmid carrying 18 telomeric repeats was digested with BsmBI restriction enzyme (New England Biolabs), followed by heat inactivation of the enzyme at 80 °C for 20 min. The resulting 4-nucleotide 5′ overhang was filled in by using Klenow exo$^-$ polymerase (New England Biolabs) and 33 μM dATP, 33 μM dTTP, and [α-^{32}P]dCTP under standard reaction conditions for 15 min at 25 °C. The reaction was stopped by addition of EDTA to a final concentration of 10 mM. Unincorporated nucleotides were removed by passing the DNA through a Sephadex G-50 column. The resulting DNA was incubated with increasing amounts of Taz1pΔC or Taz1p, respectively, for 20 min at 37 °C, and the resulting complexes were separated by electrophoresis on a 4% polyacrylamide gel in 0.5× TBE (45 mM Tris borate, 1 mM EDTA) buffer, and visualized by autoradiography.

Taz1p-DNA Incubations and Electron Microscopy—Model telomere DNAs (50–200 ng) containing different overhangs were incubated with 100 ng of Taz1p (see figure legends for details) for 2 to 20 min at room temperature in a final volume of 25 μl of buffer B (10 mM HEPES-NaOH, pH 7.5, 1 mM EDTA, 25 mM NaCl, 25 mM KCl, 10 mM 2-mercaptoethanol). To directly examine the complexes by EM, the samples were fixed by adding an equal volume of 1.2% glutaraldehyde (Sigma) for 5 min at room temperature. To remove excess protein and fixatives the samples were passed over 2-ml columns of Bio-Gel A50m equilibrated with TE. Aliquots of the fractions containing the complexes were mixed with a buffer containing spermidine for 35 s and adsorbed onto copper grids coated with thin carbon film, glow charged shortly before sample application. Following adsorption of the samples to the EM support for 2–3 min, the grids were dehydrated through a graded ethanol series and rotary shadowcast at 10^{-7} torr with tungsten (47). To stain single-stranded tails on the model telomere templates, *E. coli* SSB protein (purified in the JDG laboratory) was added to the DNA at a mass ratio of 10:1 followed by fixation and preparation for EM as above. The grids were examined using Philips CM12 or Philips/FEI Tecnai12 instruments at 40 kV. Images were collected using a Gatan 4kx4k CCD camera or sheet film. Images on film were scanned using a Nikon LS4500 film scanner and the contrast adjusted using Adobe Photoshop software. For glycerol spray/low voltage EM, the 70- and 90-kDa forms of Taz1 were exchanged using a Sephadex G-50 spin column into a buffer containing 40% glycerol and 50 mM ammonium bicarbonate, pH 7.5, and sprayed as microdroplets onto thin carbon foils. Following sublimation overnight at 1×10^{-7} torr the samples were rotary shadowcast with tungsten and examined in the Tecnai 12 at 16 KV (5).

RESULTS

Production of Full-length and C-terminal Truncated Taz1p—The fractions eluted from the nickel column contained two major bands (Fig. 1*A*, *lane 1*). Mass spectrometry analysis ("Experimental Procedures") revealed that the higher molecular weight protein corresponds to full-length Taz1 (with the hexahistidine tag), whereas the lower molecular weight species corresponds to Taz1p truncated at its C terminus (Taz1pΔC). This truncation is likely because of premature transcription termination, as coupled transcription/translation of the Taz1 gene from a PCR template yielded the same two forms and the proportion of the truncated form did not increase with time, arguing against a possibility that it is a result of specific proteolytic cleavage of the full-length Taz1p (data not shown). The truncation eliminates 107 amino acids including almost the entire Myb DNA-binding domain that is analogous to a dominant negative mutant of TRF2 (Fig. 1*B*). It would be of interest to assess a possible physiological role of regulation of Taz1p activity by producing the two forms individually in *S. pombe*.

Subjecting the mixture of Taz1p and Taz1pΔC to gel filtration on Superose 6 did not result in separation of the two forms (Fig. 1*C*). However, we observed that the protein eluted from the column together with apoferritin (440 kDa), indicating that in its native state Taz1p forms a trimer of dimers ($3 \times (2 \times 75) = 450$; see also the section "Taz1p Forms Oligomeric Donut Structures"). As the presence of Taz1pΔC in the multimeric complex may change its DNA binding properties, we developed conditions for enrichment of either of the Taz1p forms (Fig. 1*A*, *lanes 2* and 3; see "Experimental Procedures"). Testing both forms by gel-retardation assays using a DNA template carrying 18 fission yeast telomeric repeats demonstrated that in contrast to the full-length Taz1p, Taz1pΔC is unable to form a complex with the probe (Fig. 1*D*).

Generation of Model Telomere—To directly visualize Taz1p interactions with telomeric DNA *in vitro*, a model DNA containing a fixed number of 5′-GGTTACA-3′ repeats was created by expansive cloning (see "Experimental Procedures" and Ref. 24). The final plasmid construct (pLT500) carries 74 telomeric repeats (518 bp), which is about twice as long as the telomeric tract on the fission yeast chromosomes (Fig. 2). Although the strategy also yielded a plasmid with 38 repeats (266 bp) where the length of the array is more similar to that of natural telomeres, pLT500 was chosen for electron microscopic (EM) analysis because longer terminal loops would be more easily visualized by EM. As described for the human model telomere (24), 3′ terminated ss oligonucleotide tails with different lengths and sequence can be easily ligated to the end of the model DNA. Using *E. coli* SSB protein as a marker for the presence of a ssDNA tail, EM analysis revealed that >90% of the model telomere DNA molecules contained ss DNA ends.

T-loop Formation on a Model Telomere Mediated by Taz1p—The standard template used for this study contains a 49-nucleotide (nt) 3′ overhang, $(GGTTACA)_7$, ligated to the terminus of the model telomere DNA. This substrate was incubated for 20 min with Taz1p using conditions optimized by EM ("Experimental Procedures"). The presence of NaCl (≥100 mM) was required to prevent aggregation of the protein. Concentrations of nonionic detergents such as Triton X-100 even as low as 0.025% dramatically reduced the amount of protein bound. Importantly, inclusion of 10 mM 2-mercaptoethanol into the reaction increases the proportion of molecules with Taz1p bound within the telomeric track and decreases nonspecific binding.

As seen by EM the DNA was present in a variety of forms. First, a fraction of the linear DNA molecules were present with no protein bound (not shown) and the amount of Taz1p added was adjusted so that this ranged between 10 and 35% of the total. At a ratio of Taz1p to DNA of 1 μg of protein: 1 μg of DNA, the most common DNA species consisted of a model telomere with a protein particle located at the very end of the DNA (Fig. 3*A*, *upper left corner*). Although Taz1p was identified as a protein with affinity to the ds telomeric DNA of *S. pombe*, a high fraction of the molecules inspected by EM had Taz1p bound at the very end of the model telomere as opposed to internally along the telomeric tract. These results support a hypothesis that Taz1p prefers a ss/ds telomeric junction over the ds region of the telomere and that this preference might be important for a physiological role(s) of Taz1p, including t-loop formation.

The second major species consisted of model telomeres in which one end was folded back into a loop with a protein complex at the loop junction (t-loops) (Fig. 3). Measurement of the size of the loops revealed that a substantial number of loops exceeded the 500-bp length of the telomeric tract (data not shown). Whereas most of the internally bound Taz1p was

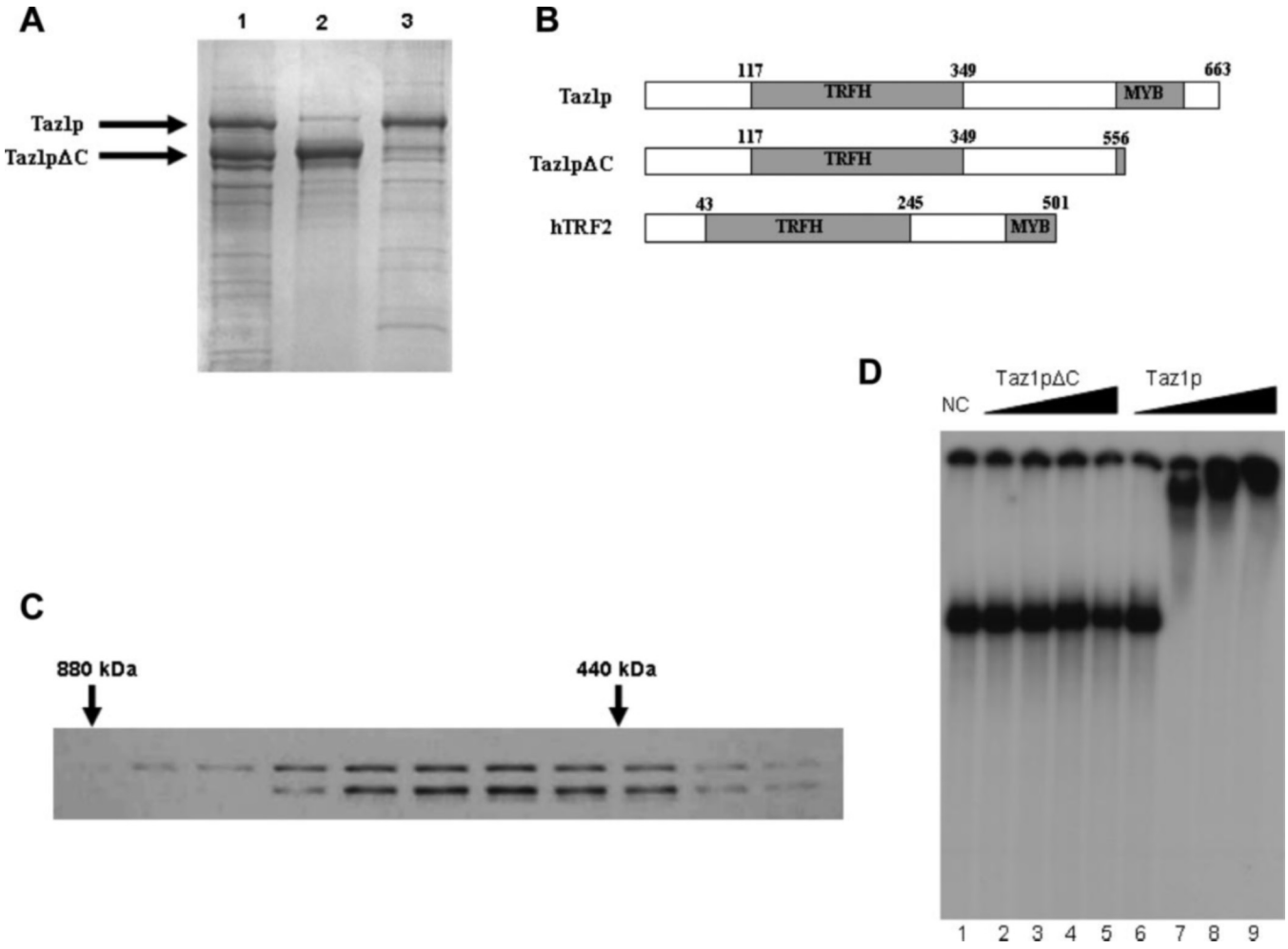

FIG. 1. **Full-length and truncated versions of Taz1p.** *A*, examples of fractions containing either both or just one of the Taz1p forms assayed by SDS-PAGE. *Lane 1*, mixture of Taz1p and Taz1pΔC; *lane 2*, purified Taz1p△C; *lane 3*, purified Taz1p. *B*, diagram of the full-length Taz1p, Taz1pΔC, and TRF2 (adapted from Ref. 37). Note that Taz1pΔC lacks almost the entire Myb-like domain responsible for DNA binding. *TRFH*, TRF homology domain. *C*, a mixture of Taz1p and Taz1pΔC was subjected to fast protein liquid chromatography gel filtration chromatography on Superose 6 ("Experimental Procedures"). The fractions were assayed for the presence of Taz1p by immunoblot using anti-penta(His) antibodies. Positions of the corresponding molecular weight standards are indicated by *arrows*. *D*, gel retardation assay for the full-length Taz1p and Taz1pΔC using the linearized plasmid containing 18 fission yeast double-stranded telomeric repeats as a probe ("Experimental Procedures"). *Lane 1*, negative control; *lanes 2–5*, Taz1pΔC (250, 750, 1250, and 2500 ng, respectively); *lanes 6–9*, full-length Taz1p (250, 750, 1250, and 2500 ng, respectively).

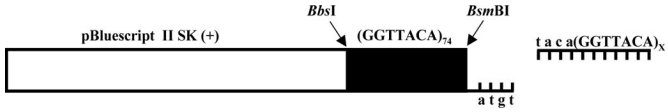

FIG. 2. **Model telomere template.** The model telomere termini were altered in the length and sequence of the overhang. Using expansive cloning as described by Stansel *et al.* (24), a tract of ~500 bp was achieved. The model telomere template, when linearized, contains a 4-nt 5′ overhang to which an oligonucleotide can be ligated to create a variety of model DNAs.

within 500 bp of an end and thus presumably bound to the telomeric DNA, in some cases Taz1p was present further in from an end and thus along the plasmid sequences. Inspection of the sequence of the pBluescript vector revealed two cryptic Taz1p-binding sites (GGTTAC) starting at positions 44 (direct strand) and 2,708 (complementary strand), respectively. This may account for some of the Taz1p binding in the plasmid sequences as well as for the loops larger than 500 bp.

When Taz1p was allowed to bind to the model telomere DNA in the presence of 2-mercaptoethanol, in more than 50% of the molecules inspected, protein particles formed an array that decorated the telomeric segment (Fig. 4). The protein formed distinct spherical balls distributed along the repeat tracts in a manner indicative of little cooperativity. This binding pattern is similar to that of hTRF1 bound to human telomeric arrays (23). The Taz1p array-covered telomeres often formed a fold-back structure (Fig. 4, *A* and *B*) suggesting that TRF1-like binding does not affect the ability of Taz1p to mediate t-loop formation. This observation goes in line with a hypothesis that as the single TRF1/TRF2 homologue, fission yeast Taz1p fulfills the functions of both TRF1 and TRF2 in remodeling the telomere.

When the template with a 49-nt $(GGTTACA)_7$ 3′ overhang was incubated with Taz1p in 2-mercaptoethanol containing buffer and 1,500 DNAs were scored 33.8 ± 8.9% had a Taz1p particle bound at one end, 13.3 ± 5.3% had one end folded back into a loop with Taz1p at the loop junction, 23.8 ± 0.3% had a Taz1p particle bound within the telomeric repeat tract, 23.3 ± 8.9% were protein-free and 5.9 ± 1.6% were scored as containing protein bound internally along the plasmid sequences (Table II).

To examine the dependence of Taz1p for its binding to different single-stranded tails on the model telomere, different oligonucleotides (Table I) were ligated to the BsmBI-linearized pLT500. Incubation of these model telomeres with Taz1p was carried out and the DNA-protein species were scored by EM

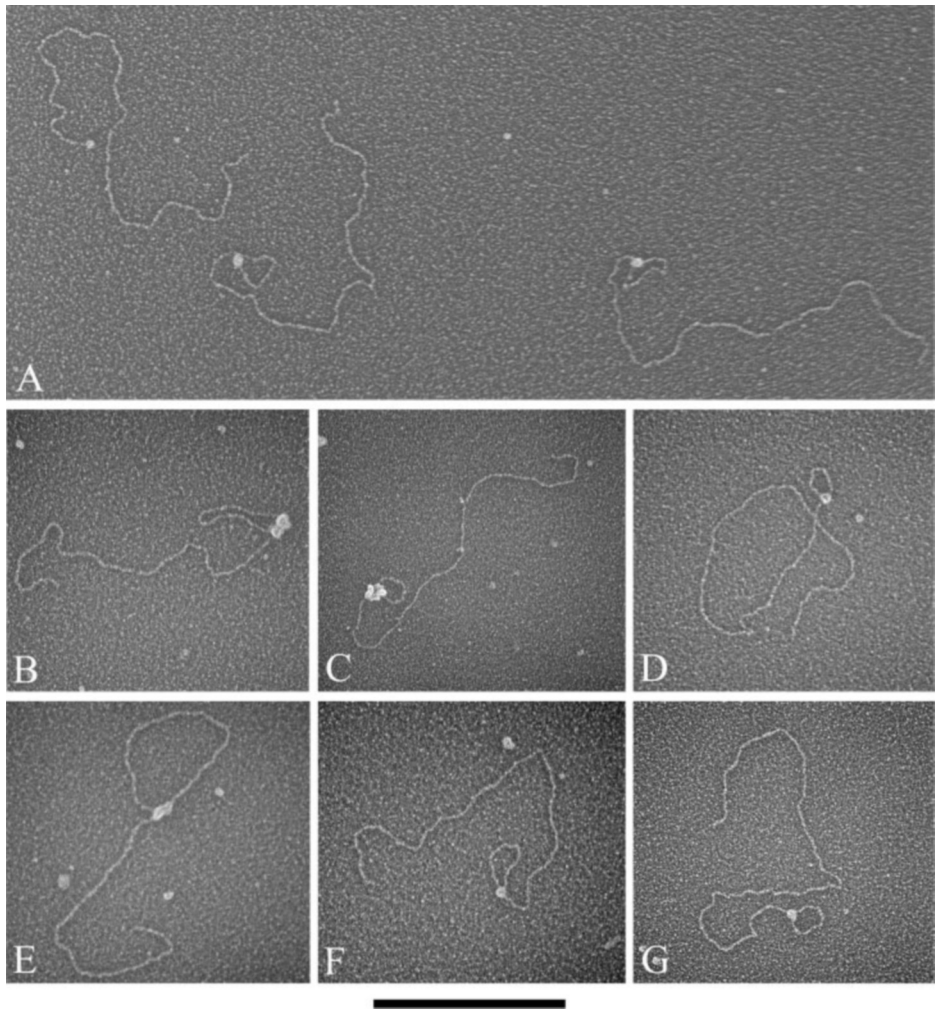

FIG. 3. **Taz1p mediates t-loop formation at the model telomere.** Taz1p was incubated with the model telomere DNA and the resulting DNA-protein complexes were prepared for EM by adsorption to thin carbon foils, dehydration, and rotary shadowcasting with tungsten ("Experimental Procedures"). Shown are examples of t-loops and one end-bound molecule (*upper left corner* in *panel A*). Shown in reverse contrast, the *bar* is equivalent to 1000 bp.

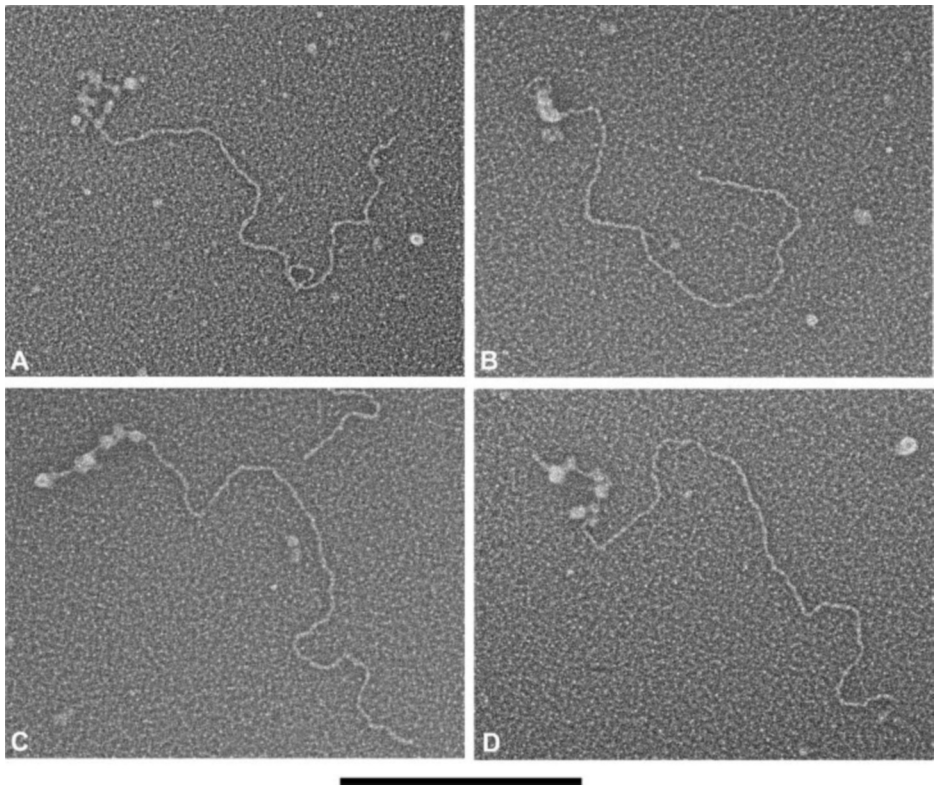

FIG. 4. **Multiple binding of Taz1p along the telomeric tract.** Incubation of Taz1p with the model telomere in a buffer containing 10 mM 2-mercaptoethanol resulted in loops covered with protein (*A*), loops with multiple protein particles at the junction (*B*), and linear chains of Taz1p covering the length of the telomeric tract including the end (*C*), or without end binding (*D*). Samples were prepared for EM as described in the legend to Fig. 3, and are shown in reverse contrast. The *bar* is equivalent to 1000 bp.

TABLE I
Oligonucleotides

SpTEL_2, SpTEL_7, and SpTEL_11 contain 2, 7, and 11 consensus telomeric repeats, respectively; SpTEL_R contains a 49-nt random sequence; SpTEL_2R contains 2 telomeric repeats followed by 35-nt random sequence; Non-tel was adopted from Ref. 35; HIS3 was adopted from Ref. 50.

Name	Sequence (5′→3′)
SpTEL_2	tacaGGTTACAGGTTACA
SpTEL_7	tacaGGTTACAGGTTACAGGTTACAGGTTACAGGTTACAGGTTACAGGTTACA
SpTEL_11	tacaGGTTACAGGTTACAGGTTACAGGTTACAGGTTACAGGTTACAGGTTACAGGTTACA
SpTEL_R	tacaGACTCTAGAGGATCCCGCTTACAGACAAGCTGTGACCGTCTCCGGGAGC
SpTEL_2R	tacaGGTTACAGGTTACACCGCTTACAGACAAGCTGTGACCGTCTCCGGGAGC
Non-tel	tacaGCTATGAATGCAGTAGTCGCGTAGTGTATCGA
HIS3	tacaCCGGTTCGTAAGGCCGACCAGCGA

TABLE II
Effect of the single-stranded overhang on the number of t-loops and the frequency and location of Taz1p binding

The percentages of the corresponding species of molecules are expressed as a fraction of the total molecules. The numbers in parentheses represent the standard deviations from one experiment to another (n = number of inspected molecules per corresponding terminal structure).

Terminal structure	total *n*	 unbound	 tip	 <500 bp	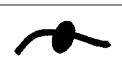 >500 bp	 t-loops
	500	17.4	25.8	50.8	4.6	1.4
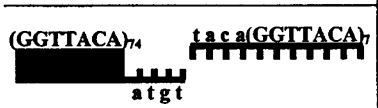	1500	23.3 (8.9)	33.8 (1.8)	23.8 (0.3)	5.9 (1.6)	13.3 (5.3)
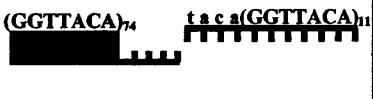	500	3.4	37.8	46.6	2.0	10.4
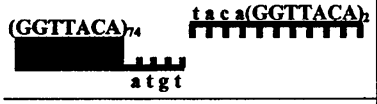	600	15.6 (3.4)	23.3 (4.7)	56.8 (1.1)	2.1 (0.1)	2.3 (2.4)
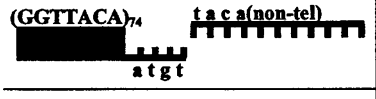	500	18.2	32.6	43.4	3.8	2.0
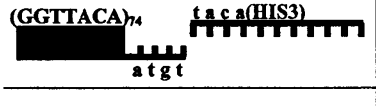	500	20.6	36.0	37.8	4.8	0.8
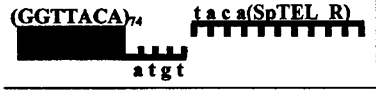	600	9.6 (0.6)	27.5 (0.7)	59.2 (1.1)	1.7 (1.0)	2.0 (0)
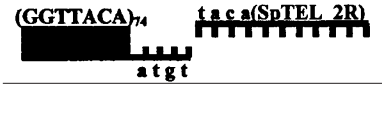	500	13.2	23.4	59.4	2.2	1.8

using the criteria as described above (Table II). From these results it is clear that Taz1p requires a ss telomeric overhang for t-loop formation. In contrast to a telomeric overhang containing 7 repeats (49 nt) and 11 repeats (77 nt), respectively, a telomeric overhang containing two repeats (14 nt) and non-telomeric overhangs were unable to promote t-loop formation. In addition, in contrast to the full-length Taz1p, Taz1pΔC exhibited very poor binding to the DNA template and only a background level of t-loops was observed (data not shown).

Taz1p Forms Oligomeric Donut Structures—Inspection of the Taz1 complexes that formed the t-loops frequently showed a single, large discrete particle at the junction of the loop and the tail (Fig. 3, *A*, *D*, *F*, and *G*) and often these particles appeared to have a donut-like appearance. A panel of such examples is shown at higher magnification in Fig. 5 (*A–D*). Indeed inspection of the Taz1 protein free of DNA on the EM substrate revealed many of these donut-like particles and their size was much larger than what would be expected from the known mass of a Taz1p homodimer (150 kDa). Furthermore, when the Taz1pΔC preparation was used, long filamentous structures were present that were absent in preparations with the full-length Taz1p (data not shown). To examine the protein by a more gentle preparative method that does not employ chemical fixation or exposure to organic solvents, preparations of Taz1p and Taz1pΔC were prepared by glycerol spray/low voltage EM ("Experimental Procedures"). Examination of the samples at 16 kV revealed oligomeric donut-like particles in the Taz1p sample (Fig. 5, *E–G*). These donuts were not present

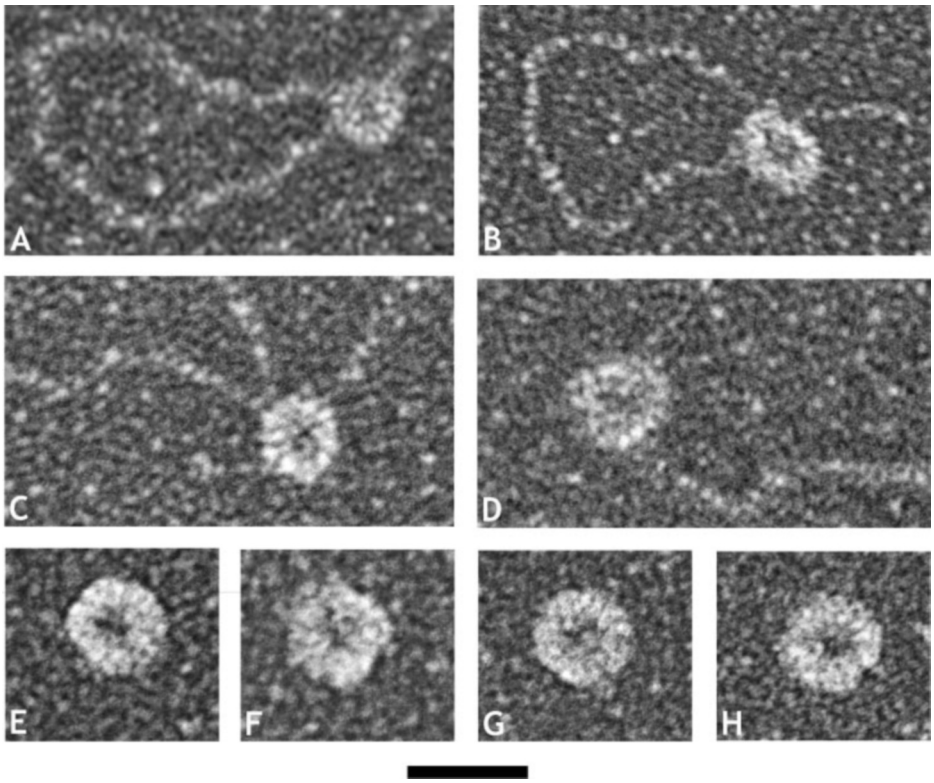

FIG. 5. **Taz1p forms donut-like oligomers.** *A–D*, enlargements of Taz1p bound to telomeric sequences in molecules prepared for EM as described in the legend to Fig. 3. Examples are shown of donut-like Taz1p oligomers at the t-loop junction (*A–C*) and at the end of a telomeric tract (*D*). Taz1p in the absence of DNA was prepared without fixation by glycerol spray/low voltage EM and 4 examples of donut oligomers are shown (*E–H*). Examples are shown in reverse contrast. The *bar* is equivalent to 26 (*A–D*) and 20 nm (*E–H*).

when Taz1pΔC was examined; rather long worm-like filaments were abundant. The size of the donut particles (width 18 nm uncorrected for metal shadowing and a hole of 3 nm) is consistent with a hexameric ring of 450 kDa. To obtain a quantitative estimate of the mass and degree of heterogeneity of the Taz1 particles, Taz1p and apoferritin (440 KDa) were prepared for EM by glycerol spray/low voltage EM side by side on separate EM grids. The projected area of 40 Taz1p particles was measured and compared with the projected area of 40 apoferritin particles. The mean projected area of the Taz1p particles was 439 ± 56 units as compared with 383 ± 34 units for apoferritin. Thus the Taz1p particles are relatively homogeneous with a projected area ~15% greater than that of the globular shaped apoferritin. A hexamer of Taz1p would be 450 kDa, very close to the mass of apoferritin. These results are highly consistent with a hexameric ring of Taz1p with a hole in the center as contrasted to other oligomeric species such as tetramers or octamers (300 and 600 kDa). These results go in line with the gel filtration experiments (Fig. 1*C*) and argue that native Taz1p may oligomerize as a trimer of dimers. In addition, the donut-like architecture of the Taz1p complex revealed by EM has implications for its function at the fission yeast telomere (see below).

DISCUSSION

The occurrence of a looped back structure, termed a t-loop, at the ends of chromosomes of a variety of organisms (5–9, 11) suggests not only its general importance for telomere maintenance, but also has exciting evolutionary implications (10). However, information about the cellular components required for their formation is still rudimentary (24, 48). A simple model system that could provide a detailed understanding of this type of telomere remodeling is needed. Although budding yeast have been extremely instrumental in telomere biology (49), they lack a homologue of TRF2, a crucial player in t-loop formation in mammalian cells. Therefore even though telomeres in *S. cerevisiae* appear to form fold-back structures (25–28), their nature and mechanism of formation may or may not be strictly analogous to t-loops in mammalian cells. On the other hand, the presence of a TRF-like protein, Taz1p, in *S. pombe* as well as similar "telomeric" phenotypes of its defective forms (35), make the fission yeast a potentially valuable model for studying t-loop dynamics.

In this study, model telomere DNAs and purified Taz1 protein were used to examine the features of Taz1p-telomere interactions. As in the case of TRF2, Taz1p induced t-loop formation when the model telomere contained a 3′ overhang with consensus telomeric repeats. Similar to TRF2, efficient Taz1p-mediated t-loop formation depended on the presence of a ss telomeric overhang. Non-telomeric ss overhangs had a limited potential for promoting both looping and Taz1p binding to the tip of the model template. This is in agreement with the observation of Vassetzky *et al.* (50) that complexes of Taz1p and a telomeric probe can be disrupted by high molar ratios of single-stranded G-rich oligonucleotides. It was also recently demonstrated that Taz1p plays a role in a double-stranded DNA break repair (43). These properties of Taz1p may reflect its potential ability to directly bind and act on double-stranded DNA breaks, in particular if the DNA end contains an extruded single strand.

Taz1p exhibits amino acid sequence homology to both TRF1 and TRF2. Its apparent preference for ss/ds telomeric junctions and a role in mediating t-loop formation is reminiscent of the binding characteristics of TRF2. On the other hand, under some conditions, Taz1p is able to form protein arrays on the telomeric repeat DNA, thus resembling TRF1 binding to human telomere (23). It was suggested that TRF1 may be involved in the early steps of folding the telomeric DNA back on itself and/or may aid in compacting the telomeric chromatin (5, 24)). As Taz1p is the only TRF-like protein in *S. pombe*, our results support its dual function (performed by TRF1 and TRF2 in mammalian cells) at fission yeast telomeres.

Glycerol spray/low voltage EM and gel filtration analysis showed that Taz1p exists in an oligomeric state in solution and both methods were in agreement that the major oligomeric

species is likely a hexamer of ~470 kDa. The EM results revealed the presence of a donut-like particle with a distinct 3-nm hole in the center. When the C terminus was truncated, Taz1pΔC, long protein filaments were abundant and their width was similar to the diameter of the donuts. Structurally rings and filaments are closely related as a filament can be composed of rings stacked one on top of the next, or by a transition between a closed flat ring and an open lock washer, the latter of which could assemble into a filamentous chain. In the case of Taz1pΔC, the truncation may facilitate this transition.

A donut-like shape of the Taz1p oligomer may be a clue to an explanation of the puzzling observations of t-loops whose sizes exceeded the length of the telomeric tract present on the model telomere. One possible scenario would be that after binding of Taz1p to the ss/ds telomeric junction and formation of the t-loop, Taz1p mediates sliding of the 3′ tail through the template DNA molecule, thus leading to the generation of loops exceeding 500 bp in size. Sliding over the entire linear molecule would then result in the tip-bound DNAs being indistinguishable from the molecules that originated from a simple binding of Taz1p to the ss/ds junction. To test this scenario one could place a barrier at the non-telomeric end of the template that should lead to a higher frequency of either loops or circles. To do this, we placed a biotin-streptavidin block at the non-telomeric end of the plasmid, and then added Taz1p. Although in some samples more than 10% circles were observed, there was a large variation between individual experiments (data not shown). Thus further work is needed to test the sliding model.

In our hands, a maximum of 10–15% of the input DNAs, as scored by EM, were assembled into t-loops by Taz1p. These values are close to those observed for TRF2-mediated t-loop formation (24). The explanations presented previously for why these values did not approach 100% (24) apply here as well. In particular, the 10–15% value likely represents equilibrium between formation and release of the loops, and other factor(s) not included in the reconstitution assay may be required for efficient t-loop formation. In addition, possible sliding of the 3′ overhang along the duplex may lead to a higher proportion of tip-bound molecules and underscoring the fraction of t-loops. At this point it is difficult to speculate what would drive these energy-dependent processes (similarly to TRF2, no requirement for nucleotide hydrolysis was observed) and what would be a physiological role of the Taz1p-dependent sliding. It was observed that fission yeast telomeres adopt a discrete non-nucleosomal chromatin structure and that this structure is disrupted in *taz1*$^{-}$ cells (35). A non-nucleosomal structure at the telomeres together with the sliding capacity of the Taz1p along the telomeric tract might be important for an establishment of t-loops. The original loop may be formed by invasion of the 3′ overhang anywhere within the telomeric tract by mechanisms described in Stansel *et al.* (24). Formation of this metastable complex may be followed by its sliding through the duplex until it is stalled by the first nucleosome marking a telomeric/subtelomeric junction (in the reconstituted system lacking any barrier, the complex slides all the way through the linear DNA). Within the cell, the maximal t-loop size would thus correspond to the length of the telomeric repeat array. This would argue that although the sizes of t-loops observed in the reconstituted system exceeded 500 bp, their *in vivo* sizes would be in agreement with the length of the telomeric tract. This may help the cell to monitor the length of its telomeres in addition to a one-dimensional "ruler" (*e.g.* analogous to that of a Rap1p-dependent counting machinery in *S. cerevisiae*) (31) also by its two-dimensional counterpart. Considering structural and functional similarities between Taz1p and TRF2 this model could also apply to higher eukaryotes. The correct adjustment of t-loops may be critical for the ability of the cell to sense and respond appropriately to the changes in telomere states (2, 51).

The results of our *in vitro* experiments do not unequivocally prove the existence of t-loops on *S. pombe* telomeres *in vivo*. The size of fission yeast telomeric tracts (<500 bp in *S. pombe versus* >5 kb in mammalian cells) and a low abundance of telomeres (6 telomeres per fission yeast cell *versus* 92 telomeres per human diploid cell) makes it difficult to quantitatively isolate *S. pombe* telomeric fragments and examine them for a presence of t-loops *in vivo* as we did in mammalian cells (5). In addition, t-loop formation may involve the participation of other proteins, such as Ku, Mre11 complex, spRap1, or Pot1, which will be included in our future experiments aimed at reconstitution of the fission yeast telosome. Nonetheless, the work described here provides a first step toward understanding telomere remodeling in fission yeast that, in addition to its evolutionary implications, may prove relevant in deciphering telomeric structure in higher eukaryotes.

Acknowledgments—We thank the members of our groups for discussions, L. Kovac (Department of Biochemistry, Comenius University, Bratislava) for helpful comments and continuous support, and E. Kutejová (Institute of Molecular Biology, Bratislava) for help with the fast protein liquid chromatography. We are particularly indebted to Julia Cooper for the gift of the Taz1p overproducing strain and their purification procedure prior to publication.

REFERENCES

1. McEachern, M. J., Krauskopf, A., and Blackburn, E. H. (2000) *Annu. Rev. Genet.* **255,** 331–358
2. Blackburn, E. H. (2000) *Nature* **408,** 53–56
3. Rhodes, D., Fairall, L., Simonsson, T., Court, R., and Chapman, L. (2002) *EMBO Rep.* **3,** 1139–1145
4. Smogorzewska, A., and de Lange, T. (2004) *Annu. Rev. Biochem.* **73,** 177–208
5. Griffith, J. D., Comeau, L., Rosenfield, S., Stansel, R. M., Bianchi, A., Moss, H., and de Lange, T. (1999) *Cell* **97,** 503–514
6. Murti, K. G., and Prescott, D. M. (1999) *Proc. Natl. Acad. Sci. U. S. A.* **96,** 14436–14439
7. Munoz-Jordan, J. L., Cross, G. A., de Lange, T., and Griffith, J. D. (2001) *EMBO J.* **20,** 579–588
8. Cesare, A. J., Quinney, N., Willcox, S., Subramanian, D., and Griffith, J. D. (2003) *Plant J.* **36,** 271–279
9. Tomaska, L., Makhov, A. M., Griffith, J. D., and Nosek, J. (2002) *Mitochondrion* **1,** 455–459
10. de Lange, T. (2004) *Nat. Rev. Mol. Cell. Biol.* **5,** 323–329
11. Nikitina, T., and Woodcock, C. L. (2004) *J. Cell Biol.* **166,** 161–165
12. Chong, L., van Steensel, B., Broccoli, D., Erdjument-Bromage, H., Hanish, J., Tempst, P., and de Lange, T. (1995) *Science* **270,** 1663–1667
13. Bilaud, T., Brun, C., Ancelin, K., Koering, C. E., Laroche, T., and Gilson, E. (1997) *Nat. Genet.* **17,** 236–239
14. Broccoli, D., Smogorzewska, A., Chong, L., and de Lange, T. (1997) *Nat. Genet.* **17,** 231–235
15. Ye, J. Z.-S., Donigian, J. R., van Overbeek, M., Loayza, D., Luo, Y., Krutchinsky, A. N., Chait, B. T., and de Lange, T. (2004) *J. Biol. Chem.* **279,** 47264–47271
16. Kim, S. H., Kaminker, P., and Campisi, J. (1999) *Nat. Genet.* **23,** 405–412
17. Smith, S., Giriat, I., Schmitt, A., and de Lange, T. (1998) *Science* **282,** 1484–1487
18. Li, B., Oestreich, S., and de Lange, T. (2000) *Cell* **101,** 471–483
19. Opresko, P. L., Von Kobbe, C., Laine, J. P., Harrigan, J., Hickson, I. D., and Bohr, V. A. (2002) *J. Biol. Chem.* **277,** 41110–41119
20. Fotiadou, P., Henegariu, O., and Sweasy, J. B. (2004) *Cancer Res.* **64,** 3830–3837
21. Ye, J. Z., Hockemeyer, D., Krutchinsky, A. N., Loayza, D., Hooper, S. M., Chait, B. T., and de Lange, T. (2004) *Genes Dev.* **18,** 1649–1654
22. Karlseder, J., Smogorzewska, A., and de Lange, T. (2002) *Science* **295,** 2446–2449
23. Griffith, J., Bianchi, A., and de Lange, T. (1998) *J. Mol. Biol.* **278,** 79–88
24. Stansel, R. M., de Lange, T., and Griffith, J. D. (2001) *EMBO J.* **20,** 5532–5540
25. Grunstein, M. (1997) *Curr. Opin. Cell Biol.* **9,** 383–387
26. Pryde, F. E., and Louis, E. J. (1999) *EMBO J.* **18,** 2538–2550
27. de Bruin, D., Kantrow, S. M., Liberatore, R. A., and Zakian, V. A. (2000) *Mol. Cell. Biol.* **20,** 7991–8000
28. de Bruin, D., Zaman, Z., Liberatore, R. A., and Ptashne, M. (2001) *Nature* **409,** 109–113
29. Shampay, J., Szostak, J. W., and Blackburn, E. H. (1984) *Nature* **310,** 154–157
30. Wang, S. S., and Zakian, V. A. (1990) *Mol. Cell. Biol.* **10,** 4415–4419
31. Marcand, S., Gilson, E., and Shore, D. (1997) *Science* **275,** 986–990
32. McEachern, M. J., Iyer, S., Fulton, T. B., and Blackburn, E. H. (2000) *Proc. Natl. Acad. Sci. U. S. A.* **97,** 11409–11414
33. Hiraoka, Y., Henderson, E., and Blackburn, E. H. (1998) *Trends Biochem. Sci.* **23,** 126

34. Park, M. J., Jang, Y. K., Choi, E. S., Kim, H. S., and Park, S. D. (2002) *Mol. Cells* **13,** 327–333
35. Cooper, J. P., Nimmo, E. R., Allshire, R. C., and Cech, T. R. (1997) *Nature* **385,** 744–747
36. Bianchi, A., Smith, S., Chong, L., Elias, P., and de Lange, T. (1997) *EMBO J.* **16,** 1785–1794
37. Fairall, L., Chapman, L., Moss, H., de Lange, T., and Rhodes, D. (2001) *Mol. Cell* **8,** 351–361
38. Chikashige, Y., Ding, D. Q., Imai, Y., Yamamoto, M., Haraguchi, T., and Hiraoka, Y. (1997) *EMBO J.* **16,** 193–202
39. Cooper, J. P., Watanabe, Y., and Nurse, P. (1998) *Nature* **392,** 828–831
40. Nimmo, E. R., Pidoux, A. L., Perry, P. E., and Allshire, R. C. (1998) *Nature* **392,** 825–828
41. Sadaie, M., Naito, T., and Ishikawa, F. (2003) *Genes Dev.* **17,** 2271–2282
42. Ferreira, M. G., and Cooper, J. P. (2001) *Mol. Cell* **7,** 55–63
43. Miller, K. M., and Cooper, J. P. (2003) *Mol. Cell* **11,** 303–313
44. Chikashige, Y., and Hiraoka, Y. (2001) *Curr. Biol.* **11,** 1618–1623
45. Laemmli, U. K. (1970) *Nature* **227,** 680–685
46. Borchers, C., Peter, J. F., Hall, M. C., Kunkel, T. A., and Tomer, K. B. (2000) *Anal. Chem.* **72,** 1163–1168
47. Griffith, J. D., and Christiansen, G. (1978) *Annu. Rev. Biophys. Bioeng.* **7,** 19–35
48. Stansel, R. M., Subramanian, D., and Griffith, J. D. (2002) *J. Biol. Chem.* **277,** 11625–11628
49. Zakian, V. A. (1996) *Annu. Rev. Genet.* **30,** 141–172
50. Vassetzky, N. S., Gaden, F., Brun, C., Gasser, S. M., and Gilson, E. (1999) *Nucleic Acids Res.* **27,** 4687–4694
51. Blackburn, E. H. (2001) *Cell* **106,** 661–673